JACS
JOURNAL OF THE AMERICAN CHEMICAL SOCIETY

Communication

pubs.acs.org/JACS

Template Synthesis of Gold Nanoparticles with an Organic Molecular Cage

Ryan McCaffrey,[†] Hai Long,[‡] Yinghua Jin,[†] Aric Sanders,[§] Wounjhang Park,[⊥] and Wei Zhang*[,†]

[†]Department of Chemistry and Biochemistry, and [⊥]Department of Electrical, Computer and Energy Engineering, University of Colorado, Boulder, Colorado 80309, United States

[‡]National Renewable Energy Laboratory, Golden, Colorado 80401, United States

[§]National Institute of Standards and Technology, Boulder, Colorado 80305, United States

Supporting Information

ABSTRACT: We report a novel strategy for the controlled synthesis of gold nanoparticles (AuNPs) with narrow size distribution (1.9 ± 0.4 nm) through NP nucleation and growth inside the cavity of a well-defined three-dimensional, shape-persistent organic molecular cage. Our results show that both a well-defined cage structure and pendant thioether groups pointing inside the cavity are essential for the AuNP synthesis.

The size-dependent optical and electronic properties of gold nanoparticles (AuNPs) have long been of interest in the context of nanoscience and nanotechnology.[1] In particular, AuNPs with diameters in the sub-nanometer to ∼2 nm range are known to exhibit properties that are quite unique compared to those larger than 5 nm,[2] an observation that has motivated intense interest in the design of organic architectures for the template synthesis of 1−2 nm AuNPs that can be further used in catalysis,[3] sensor devices,[4] and nanoelectronics.[5] For instance, the integration of AuNPs into electronic devices will require the use of 1−2 nm particles.[6] Since the advent of the Brust−Schiffrin method,[7] there has been a wealth of literature exploring the structure−function relationships of ligand-stabilized NPs that can be rationally designed for fundamental studies and practical applications.[8] To date, control over NP size, shape, and distribution has advanced through the use of small organic ligands, dendritic architectures, or polymers as templates or stabilizers.[1c,3b,9] Despite this recent progress, there still remain very few examples of passivating ligands allowing for a size-controlled synthesis of AuNPs.

Well-defined, discrete organic molecular cages have attracted tremendous attention[10] due to their shape persistence, structural tunability, and thermal and chemical stability. Our group has demonstrated the modular synthesis[11] of a variety of organic molecular cages and their great potential in carbon capture[12] and fullerene separation applications.[13] Furthermore, modular synthesis allows for judicious external functionalization so that molecular cages can be covalently assembled into ordered networks through the bottom-up "cage-to-framework" approach.[14] We envision that discrete rigid organic molecular cages with multiple Au-binding sites inside the cavity can serve as templates for controlled synthesis of AuNPs. Such a cage template has a well-defined architecture with a spatially confined cavity that is large enough to accommodate NPs. Compared to conventional small organic or macromolecular ligands, which form thick, insulating layers on the AuNP surface, a cage template can provide a protecting shell with minimum coverage and greater encapsulated AuNP surface accessibility. Another potential advantage of such a "cage-template" approach is that exterior functionalization on the cage may enable further assembly of AuNPs in a controlled fashion as possible three-dimensional building blocks for chemically directed hierarchical assembly, which would provide a powerful platform for development of novel nanostructured materials for optical or catalytic applications. Herein, we report the first example of size-controlled synthesis of AuNPs using a discrete organic molecular cage as a template.

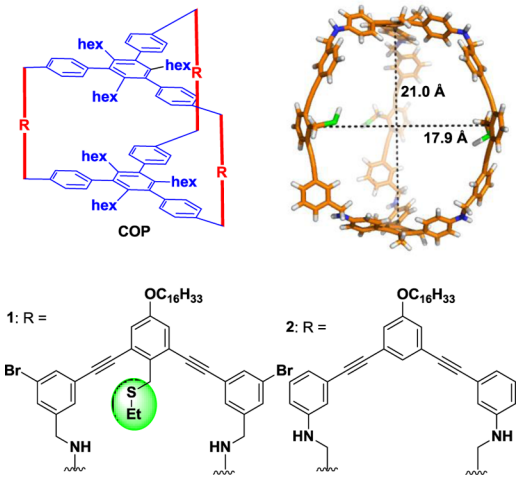

Figure 1. Structures of cages **1** and **2**, and side view of a fully stretched model of cage **1**. Methyl group for hexyl chain, and hydrogen for $OC_{16}H_{33}$ and Br were used in the calculation for simplification.

We designed trigonal prismatic cage **1** with internal cavity size of 1.8−2.1 nm (Figure 1), the interior of which is functionalized with three thioether groups. We chose to use thioether as the nucleation site for the Au deposition since it has higher stability than thiol yet is known to coordinate, albeit weakly, gold colloids.[9g,15] AuNPs of a size similar to the cage are expected to grow inside the cavity, leading to the formation of a core/shell structure, with AuNP as the core and the cage molecule as the

Received: December 11, 2013

   dx.doi.org/10.1021/ja412606t | J. Am. Chem. Soc. XXXX, XXX, XXX−XXX

Scheme 1. Synthesis of Molecular Cage 1

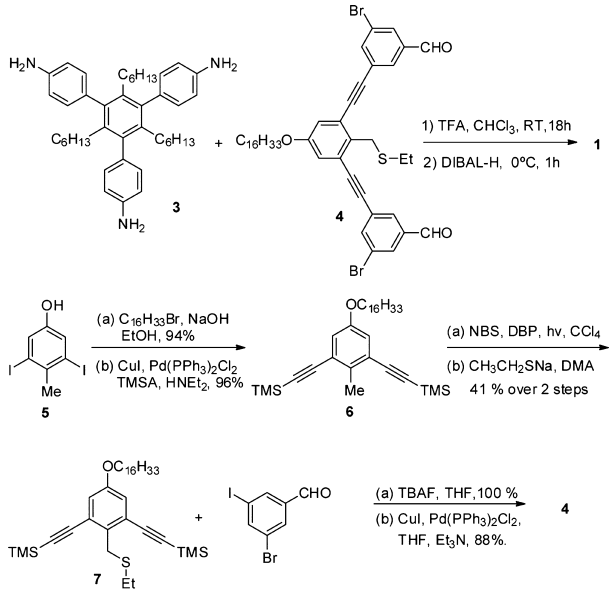

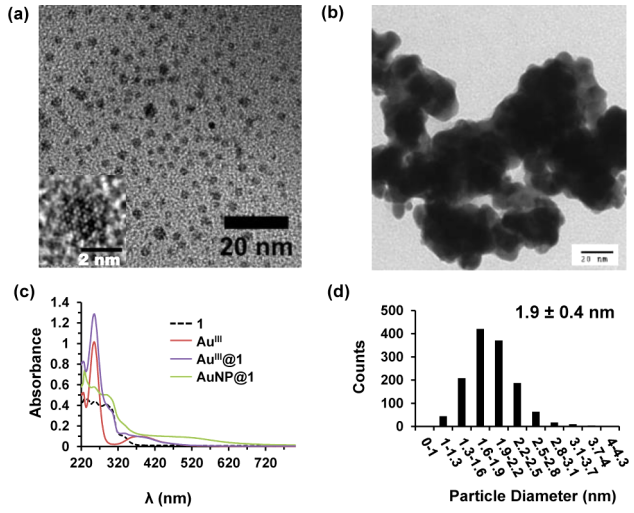

Figure 2. Top: TEM micrographs (scale bar 20 nm; inset scale bar 2 nm) of AuNP@**1** complex (a) and AuNPs produced using **2** as a ligand (b). Bottom: UV−vis absorption spectra of gold complexes in CH_2Cl_2 (c) and the size distribution of AuNP@**1** complex (d).

shell. Previously reported cage **2**, with the same cavity size but lacking thioether anchoring groups, was selected as a control compound.[12a]

Cage **1** was synthesized through dynamic imine chemistry using triamine **3** as the top and bottom panels and dialdehyde **4** with a thioether group as the three lateral edges (Scheme 1). Triamine **3** was prepared as previously described in the literature.[12b] Dialdehyde **4** was synthesized starting with 3,5-diiodo-*p*-cresol **5**, which was prepared from *p*-cresol.[16] Following alkylation of compound **5**, trimethylsilyl-protected terminal acetylenes were introduced before radical bromination at the methyl position. The brominated intermediate is critical in that it allows for the later introduction of pendant interior thioether groups. Desilylation of compound **7** followed by Sonogashira coupling with 3-bromo-5-iodobenzaldyhyde yielded the lateral side piece **4**. Imine condensation between the two building blocks **3** and **4** and subsequent reduction led to the formation of **1**. Cage **1** was characterized by ^{1}H and ^{13}C NMR, GPC, and MALDI-MS.

We used a two-phase liquid−liquid approach developed by Brust et al., with tetraoctylammonium bromide (TOAB) as a phase-transfer reagent, to prepare cage-encapsulated AuNPs.[10] A solution of TOAB in CH_2Cl_2 was added to an aqueous solution of $HAuCl_4$ (10 equiv) and stirred until the aqueous layer was colorless, indicating all $AuCl_4^-$ was transferred to the organic phase. A solution of **1** (1 equiv) in CH_2Cl_2 was added to the above biphasic mixture. Upon mixing, no obvious color change was observed in the organic phase. The mixture was subsequently reduced with an aqueous solution of sodium borohydride (190 equiv, rt). The organic phase immediately changed color from orange-red to dark brown without any precipitates, indicating efficient Au^{3+} reduction and further stabilization of the resulting AuNPs by cage molecule **1**. The organic layer containing AuNP@**1** complex was separated, and AuNP@**1** complex was precipitated from ethanol and collected by centrifugation. The AuNP@**1** complex shows good solubility in common organic solvents. The AuNPs were characterized by UV−vis, ^{1}H NMR, DOSY, TGA, and TEM.

The UV−vis absorption spectra of the solution before and after reduction are shown in Figure 2c. All the absorption measurements were performed in CH_2Cl_2 at the same concentration (1.4 μM). In the absence of cage **1**, the absorption spectrum of tetrabutylammonium tetrachloroaurate(III) in CH_2Cl_2 shows absorption peaks at λ = 250 nm, and 380 nm, arising from the ligand-to-metal charge-transfer transition (Au^{III}, red line, Figure 2c). Upon addition of the cage molecule to the Au^{3+} solution, the absorption of **1** appeared as a shoulder band in the region around 275−381 nm, and the intensity of the peak at 380 nm was decreased (Au^{III}@**1**, purple line, Figure 2c). Complete reduction of $AuCl_4^-$ to zerovalent Au and formation of AuNPs with diameter ∼2 nm were confirmed by the disappearance of the 250 nm band and the emergence of a featureless broad tail extending to 700 nm after the reduction (AuNP@**1**, green line).

The particle diameter and size distribution were analyzed using TEM images. All the samples were prepared using a solution of AuNP@**1** in CH_2Cl_2. The solution was drop-cast onto carbon-coated 300 mesh copper grids (CF300-Cu) and allowed to air-dry before the measurements. The TEM image (Figure 2a) of AuNP@**1** shows the formation of well-dispersed AuNPs with average diameters of 1.9 nm, which matches well with the estimated cage internal cavity size of 1.8−2.1 nm.

Thermal gravimetric analysis (TGA, Figure S5) shows a mass loss of 56% for pure cage **1** and a mass loss of 6% for AuNP@**1** complex between ambient temperature and 480 °C. Based on the above mass loss determined by TGA, we calculate that each cage molecule contains a NP composed of roughly 150 Au atoms. This corresponds to a 1.7 nm AuNP, which is in close agreement with the AuNP size observed by TEM.

Despite its small size, AuNP@**1** complex shows excellent stability. It is stable in solutions, with no evidence of agglomeration, and without noticeable color change, over periods of several months. More importantly, it can be evaporated to dryness overnight under high vacuum and then redissolved in common organic solvents with no signs of aggregation. It should be noted that redispersion of AuNPs after drying has been difficult for AuNPs with weaker binding ligands, such as some carboxylates and multivalent thioether ligands.[9h,17] Presumably, the cage shell provides good solubility as well as effective coverage and protection of the AuNPs' surface, thus

dx.doi.org/10.1021/ja412606t | J. Am. Chem. Soc. XXXX, XXX, XXX−XXX

preventing their aggregation. The high solubility and stability of the AuNP@**1** complex further support the notion that NPs reside inside the cage cavity.

In the ^{1}H NMR spectra of the above AuNP@**1** complex, we did not observe the phase-transfer agent TOAB (Figure S1). Interestingly, substantial broadening and shifting of not only the protons of the thioether group but also all aromatic protons of the cage skeleton were observed. This is in great contrast to the oligomeric ligands based on benzylic thioethers reported by Simon and Mayor, in which no significant shifting and broadening of proton signals of ligands were observed upon the formation of AuNP complex.[9f,15b] Line broadening of resonances is characteristic for ligands with thiol functionality, which have the highest affinity to Au.[18] Line broadening commonly occurs due to the intrinsic heterogeneous environment for the bound ligands on the AuNPs and their restricted mobility on the NP surface.[17] The considerable line broadening and shifting of almost all protons of the cage skeleton in the present case therefore support the notion that the cage shell is likely tightly wrapped around the AuNP, and experiences restricted mobility and fast spin relaxation.

It has been known that multidentate thioether ligands, such as thioether dendrimers, can stabilize AuNPs to form stable and narrowly dispersed ligand-wrapped NPs.[9f,15b,19] To further corroborate that the particle rests inside of the cage cavity and rule out the possibility of particle formation through aggregation of multiple cages on the AuNP surface, ^{1}H diffusion-ordered spectroscopy (DOSY) NMR was performed on both free cage **1** and AuNP@**1** under the same temperature and concentration (Figures S3 and S4). As expected, we obtained very similar diffusion coefficients for cage **1** and AuNP@**1**, 2.5 and 2.4 respectively, which indicates the similar size and shape of free cage and AuNP@**1**. This study provides additional evidence supporting that AuNP formation is a result of a single cage encapsulation rather than intercage interactions and the simple multivalency effect of ligands.

To further confirm the role of cage scaffold and thioether groups in AuNP synthesis, we conducted two control experiments using cage **2**, which lacks thioether groups, and thioether ligand **4**, which lacks a cavity. First, $HAuCl_4$ was reduced in the presence of **2**, a structural analogue of cage **1** but without the three internal thioether groups. As expected, upon reduction with $NaBH_4$, we observed the immediate and complete precipitation of aggregated NPs under conditions similar to those used to form AuNP@**1** complex. The TEM image of AuNPs obtained from the control experiment with **2** (Figure 2b) showed only shapeless agglomerates, indicating that **2** is unable to serve as a template for the synthesis of AuNPs, presumably due to the lack of nucleation (i.e., Au binding) sites. In the other control experiment, the side piece **4**, which bears a thioether group, was used as the ligand. In this case, we observed similar rapid aggregation and precipitation of AuNPs upon reduction, suggesting the poor stabilization of AuNPs by monodentate open ligand **4**.

It is therefore tempting to conclude that both the thioether groups and the closed cage structure itself are playing critical roles in controlled AuNP synthesis. The thioether groups serve as the initial nucleation sites for AuNP growth and also stabilize the resulting NP. Once seeded, the Au nanocluster grows until it is confined sterically within the cage, and the three thioether groups and the six amino groups may provide stabilization through Au surface binding. The fact that the AuNP@**1** complexes themselves remain isolated from one another is likely due to the long alkyl chains present around the cage exterior. The working mechanism of this cage template is very different from that of the previously reported dendrimer template, which inherently relies on multipoint interactions that conform to the surface of the particle, thus allowing it to grow until "dendritic wrapping" of the cluster becomes favorable.[9f]

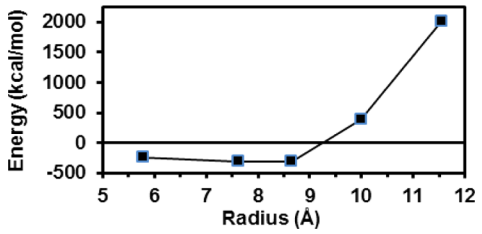

Figure 3. Energy of cage **1** as a function of encapsulated nanoparticle radius.

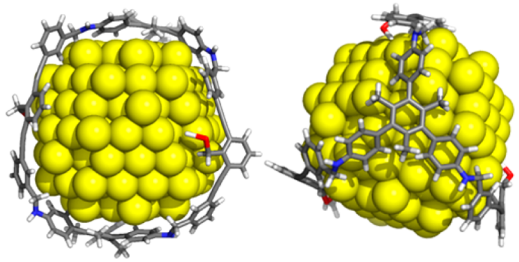

Figure 4. Calculated energy-minimized structure of AuNP@**1**. AuNP radius is 8.65 Å.

Computational simulation of the interaction between cage **1** and AuNPs of different radii provides theoretical support for our experimental findings. The AuNPs were generated using a Au crystal cubic close-packed lattice structure with a closest Au−Au separation of 0.2884 nm. Five different AuNPs are used, with radii of 11.54, 9.99, 8.65, 7.63, and 5.77 Å, respectively. For each NP, we built a cage around it and bonded the three sulfur atoms of the cage to the Au atoms at the equator of the NP, 120° apart. The Amber 11.0 molecular dynamics program package[20] was then used to optimize the structures of the cage/NP complexes. The force field used for the cage was the general Amber force field (GAFF)[21] with the charge parameters computed by the AM1-BCC method,[22] and the force field for gold was adopted from Agrawal et al.[23] For each optimization run, the atoms on AuNPs were frozen, and the structure of the cage was optimized. The cage was first minimized for 5000 steps using the conjugate gradient method, and then it was further optimized by the simulated annealing method for 150 ps with a time step of 1 fs. During the simulated annealing, the system temperature was first raised to 1000 K for 50 ps and then gradually cooled to 0 K over another 100 ps. Finally, the annealed structure was minimized again for another 5000 conjugate gradient steps. The total energy of cage/cage and cage/gold interactions was calculated on the basis of the energy-minimized structure. Figure 3 shows the cage energy as a function of the encapsulated NP radius. The energy first decreases when the radius increases due to the larger van der Waals attraction between the cage and the NP. At a radius of 8.65 Å (1.7 nm diameter), the energy reaches the minimum, and the structure of the AuNP@**1** complex is presented in Figure 4. This is in close agreement with the 1.9 ± 0.4 nm average diameter we observed experimentally through the TEM characterization.

In summary, we have demonstrated a novel cage-templated strategy for the controlled synthesis of AuNPs through the use of

dx.doi.org/10.1021/ja412606t | J. Am. Chem. Soc. XXXX, XXX, XXX−XXX

a well-defined, discrete organic molecular cage functionalized with pendant interior thioether groups. The AuNPs formed inside the cage cavity exhibit narrow particle size distribution (1.9 ± 0.4 nm) and could potentially be used as seed particles for further seed-mediated growth of nonspherical Au nanocrystals. The average particle size obtained from this cage-templated synthesis is consistent with the molecular dynamics simulation results. To the best of our knowledge, this is the first example of *in situ* AuNP growth in a confined organic molecular environment. Our results show that the successful controlled synthesis of AuNPs is attributed to the combination of a well-defined cage scaffold and the interaction between AuNPs and pendant thioether groups that serve as the nucleation and stabilization sites for AuNPs grown inside the cage. The diversity in size and shape of cage molecules makes such a cage-template approach a versatile strategy for synthesis of AuNPs with tunable size and shape. Hierarchical NP assembly with special optical or magnetic properties can be achieved by the proper functionalization of cage exterior, which can direct their spatial arrangement. Furthermore, the abundance of available surface area from the resulting AuNPs would allow for their facile interactions with small molecules, thus making AuNP@**1** an interesting model complex for homogeneous catalysis. Currently the scope of this cage-template strategy in NP synthesis as well as utilization of exterior functionalized molecular cages to direct AuNP assembly are being investigated in our laboratory and will be reported in due course.

■ ASSOCIATED CONTENT

Ⓢ Supporting Information

Experimental procedures, GPC, TGA, TEM images, NMR spectroscopic data, and theoretical calculations. This material is available free of charge via the Internet at http://pubs.acs.org.

■ AUTHOR INFORMATION

Corresponding Author

wei.zhang@colorado.edu

Notes

The authors declare no competing financial interest.

■ ACKNOWLEDGMENTS

The authors thank Army Research Office (W911NF-12-1-0581) for financial support, Dr. Tom Giddings and Suehyun Cho for TEM image analysis, and Dr. Richard Shoemaker for NMR analysis, and Dr. Matthew Cowan for TGA study. This research used capabilities of the National Renewable Energy Laboratory Computational Sciences Center, which is supported by the Office of Energy Efficiency and Renewable Energy of the U.S. Department of Energy under Contract No. DE-AC36-08GO28308.

■ REFERENCES

(1) (a) Rosi, N. L.; Mirkin, C. A. *Chem. Rev.* **2005**, *105*, 1547. (b) Jiang, D. E. *Nanoscale* **2013**, *5*, 7149. (c) Zhao, P. X.; Li, N.; Astruc, D. *Coord. Chem. Rev.* **2013**, *257*, 638. (d) Daniel, M. C.; Astruc, D. *Chem. Rev.* **2004**, *104*, 293. (e) Grzelczak, M.; Vermant, J.; Furst, E. M.; Liz-Marzan, L. M. *ACS Nano* **2010**, *4*, 3591.

(2) (a) Jin, R. C. *Nanoscale* **2010**, *2*, 343. (b) Aikens, C. M. *J. Phys. Chem. Lett.* **2011**, *2*, 99.

(3) (a) Helms, B.; Frechet, J. M. J. *Adv. Synth. Catal.* **2006**, *348*, 1125. (b) Myers, V. S.; Weir, M. G.; Carino, E. V.; Yancey, D. F.; Pande, S.; Crooks, R. M. *Chem. Sci.* **2011**, *2*, 1632. (c) Astruc, D.; Liang, L. Y.; Rapakousiou, A.; Ruiz, J. *Acc. Chem. Res.* **2012**, *45*, 630.

(4) Lim, S. I.; Zhong, C. J. *Acc. Chem. Res.* **2009**, *42*, 798.

(5) Homberger, M.; Simon, U. *Philos. Trans. R. Soc. A* **2010**, *368*, 1405.

(6) Schmid, G.; Simon, U. *Chem. Commun.* **2005**, 697.

(7) Brust, M.; Walker, M.; Bethell, D.; Schiffrin, D. J.; Whyman, R. *J. Chem. Soc., Chem. Commun.* **1994**, 801.

(8) (a) Scott, R. W. J.; Wilson, O. M.; Crooks, R. M. *J. Phys. Chem. B* **2005**, *109*, 692. (b) Thompson, D.; Hermes, J. P.; Quinn, A. J.; Mayor, M. *Acs Nano* **2012**, *6*, 3007. (c) Westerlund, F.; Bjornholm, T. *Curr. Opin. Colloid Interface Sci.* **2009**, *14*, 126. (d) Whitesides, G. M.; Grzybowski, B. *Science* **2002**, *295*, 2418. (e) Whitesides, G. M.; Kriebel, J. K.; Mayers, B. T. In *Nanoscale Assembly*; Huck, W. T. S., Ed.; Springer: New York, 2005; p 217.

(9) (a) Esumi, K.; Suzuki, A.; Yamahira, A.; Torigoe, K. *Langmuir* **2000**, *16*, 2604. (b) Grohn, F.; Bauer, B. J.; Akpalu, Y. A.; Jackson, C. L.; Amis, E. J. *Macromolecules* **2000**, *33*, 6042. (c) Crooks, R. M.; Zhao, M. Q.; Sun, L.; Chechik, V.; Yeung, L. K. *Acc. Chem. Res.* **2001**, *34*, 181. (d) Vassilieff, T.; Sutton, A.; Kakkar, A. K. *J. Mater. Chem.* **2008**, *18*, 4031. (e) Boisselier, E.; Diallo, A. K.; Salmon, L.; Ornelas, C.; Ruiz, J.; Astruc, D. *J. Am. Chem. Soc.* **2010**, *132*, 2729. (f) Hermes, J. P.; Sander, F.; Peterle, T.; Urbani, R.; Pfohl, T.; Thompson, D.; Mayor, M. *Chem.—Eur. J.* **2011**, *17*, 13473. (g) D'Aleo, A.; Williams, R. M.; Osswald, F.; Edamana, P.; Hahn, U.; van Heyst, J.; Tichelaar, F. D.; Vogtle, F.; De Cola, L. *Adv. Funct. Mater.* **2004**, *14*, 1167. (h) Kim, Y. G.; Oh, S. K.; Crooks, R. M. *Chem. Mater.* **2004**, *16*, 167. (i) Shan, J.; Tenhu, H. *Chem. Commun.* **2007**, 4580.

(10) (a) Holst, J. R.; Trewin, A.; Cooper, A. I. *Nat. Chem.* **2010**, *2*, 915. (b) Cooper, A. I. *Angew. Chem., Int. Ed.* **2011**, *50*, 996. (c) Jin, Y.; Zhu, Y.; Zhang, W. *CrystEngComm* **2013**, *15*, 1484. (d) Mastalerz, M. *Angew. Chem., Int. Ed.* **2010**, *49*, 5042. (e) Rue, N. M.; Sun, J. L.; Warmuth, R. *Isr. J. Chem.* **2011**, *51*, 743.

(11) Jin, Y. H.; Jin, A.; McCaffrey, R.; Long, H.; Zhang, W. *J. Org. Chem.* **2012**, *77*, 7392.

(12) (a) Zhang, W.; Jin, Y. H.; Voss, B. A.; Jin, A.; Long, H.; Noble, R. D. *J. Am. Chem. Soc.* **2011**, *133*, 6650. (b) Jin, Y.; Voss, B. A.; Noble, R. D.; Zhang, W. *Angew. Chem., Int. Ed.* **2010**, *49*, 6348.

(13) Zhang, C. X.; Wang, Q.; Long, H.; Zhang, W. *J. Am. Chem. Soc.* **2011**, *133*, 20995.

(14) Jin, Y. H.; Voss, B. A.; McCaffrey, R.; Baggett, C. T.; Noble, R. D.; Zhang, W. *Chem. Sci.* **2012**, *3*, 874.

(15) (a) Li, X. M.; de Jong, M. R.; Inoue, K.; Shinkai, S.; Huskens, J.; Reinhoudt, D. N. *J. Mater. Chem.* **2001**, *11*, 1919. (b) Peterle, T.; Leifert, A.; Timper, J.; Sologubenko, A.; Simon, U.; Mayor, M. *Chem. Commun.* **2008**, 3438.

(16) Datta, R. L.; Prosad, N. *J. Am. Chem. Soc.* **1917**, *39*, 441.

(17) Leifert, A.; Pan-Bartnek, Y.; Simon, U.; Jahnen-Dechent, W. *Nanoscale* **2013**, *5*, 6224.

(18) (a) Terrill, R. H.; Postlethwaite, T. A.; Chen, C. H.; Poon, C. D.; Terzis, A.; Chen, A. D.; Hutchison, J. E.; Clark, M. R.; Wignall, G.; Londono, J. D.; Superfine, R.; Falvo, M.; Johnson, C. S.; Samulski, E. T.; Murray, R. W. *J. Am. Chem. Soc.* **1995**, *117*, 12537. (b) Hostetler, M. J.; Wingate, J. E.; Zhong, C. J.; Harris, J. E.; Vachet, R. W.; Clark, M. R.; Londono, J. D.; Green, S. J.; Stokes, J. J.; Wignall, G. D.; Glish, G. L.; Porter, M. D.; Evans, N. D.; Murray, R. W. *Langmuir* **1998**, *14*, 17.

(19) Peterle, T.; Ringler, P.; Mayor, M. *Adv. Funct. Mater.* **2009**, *19*, 3497.

(20) Case, D. A.; Darden, T. A.; Cheatham, T. E., III; Simmerling, C. L.; Wang, J.; Duke, R. E.; Luo, R.; Walker, R. C.; Zhang, W.; Merz, K. M.; Roberts, B.; Wang, B.; Hayik, S.; Roitberg, A.; Seabra, G.; Kolossváry, I.; Wong, K. F.; Paesani, F.; Vanicek, J.; Liu, J.; Wu, X.; Brozell, S. R.; Steinbrecher, T.; Gohlke, H.; Cai, Q.; Ye, X.; Wang, J.; Hsieh, M.-J.; Cui, G.; Roe, D. R.; Mathews, D. H.; Seetin, M. G.; Sagui, C.; Babin, V.; Luchko, T.; Gusarov, S.; Kovalenko, A.; Kollman, P. A. *AMBER 11*; University of California, San Francisco, 2010.

(21) Wang, J. M.; Wolf, R. M.; Caldwell, J. W.; Kollman, P. A.; Case, D. A. *J. Comput. Chem.* **2004**, *25*, 1157.

(22) Jakalian, A.; Bush, B. L.; Jack, D. B.; Bayly, C. I. *J. Comput. Chem.* **2000**, *21*, 132.

(23) Agrawal, P. M.; Rice, B. M.; Thompson, D. L. *Surf. Sci.* **2002**, *515*, 21.